

A graphical user interface for flexible CARS spectral library generation

MICHAEL HART,^{1*} CHRIS KLIEWER²

¹*Physics Department, California State University - Chico, 940 W. First Street, Chico, CA 95929, USA*

²*Combustion Research Facility, Sandia National Laboratory, 7011 East Ave, Livermore, CA 94550, USA*

**mhart1@csuchico.edu*

Abstract: Spectral library generation is a technique to produce libraries of theoretical spectra that are used to analyze experimental spectra gathered from femtosecond/picosecond Coherent anti-Stokes Raman scattering (fs/ps CARS). However, managing the library generation code for several molecular species and varying experimental parameters is a daunting task. To address this issue, we built a graphical user interface (GUI) that gives users the flexibility to adjust experimental parameters; while combining many iterations of the code into one, easily distributed program. We adapted the existing code to consolidate it all into one program while focusing on providing users with a robust and flexible way to generate theoretical libraries. Future work can be done to include support for additional molecular species, add quality-of-life features, and verify the accuracy of the spectra produced by the program for high pressures.

1. Introduction

Coherent anti-Stokes Raman scattering (CARS) is a third-order non-linear optical effect where probe photons scatter inelastically from a molecule after it was excited to a higher energy level. A technique known as rotational femtosecond/picosecond CARS [1,2] uses a pump and Stokes pulse to drive a transition of a molecule's rotational energy such that the scattered photon has energy equal to this transition. Since the rotational transition frequencies of many molecules fall within a narrow spectral range, unlike vibrational transition frequencies, a pump/Stokes pulse can drive multiple transitions within a macroscopic gas phase sample at once making concentration measurements possible. This in-situ technique produces spectrum that give information about the properties of gas phase samples, such as temperature and the concentration. CARS is used in the development of materials for rocket reentry into planets with thick atmospheres and to measure temperatures and concentrations inside combustion environments due to the in-situ nature of CARS. The CARS technique is also used to probe the energy transfer dynamics of larger molecules, such as CO₂ [3].

The spectra gathered by rotational femtosecond/picosecond CARS are fit against theoretical spectra to extract information about the sample. This is done by generating a large number of spectra with each one having slightly different parameters. The experimental spectrum is fit against an entire library of theoretical CARS spectra. This process is known as spectral library generation. The model used to calculate and generate the theoretical spectra is discussed at length in this paper, however, the process of fitting the experimental spectrum isn't.

Previously, the model was adapted many times to provide functionality for

more and more molecular species, and this functionality was dispersed among many code files. While this was no more than an inconvenience for the group who created it [4], distributing the model to other researchers proved to be a difficult process. There also wasn't a good way to adjust parameters besides sifting through lines of code. Our task was to consolidate the model into a single program, adapt the model to provide increased flexibility, and create a graphical user interface (GUI) that allows users to adjust parameters easily.

In this paper, we give a brief overview of the theory of molecular energy levels that is used to accurately model CARS spectra. We then discuss a function that is the main component needed to generate CARS spectral libraries. Lastly, we give a discussion of the main features and considerations of the program, including the focus on flexibility, robustness, and making universal distribution possible.

2. Theoretical Background

This section provides the theoretical background for two simple models of a diatomic molecule, the harmonic oscillator and the rigid rotator, which describe vibrational and rotational energies, respectively. Corrections are implemented to account for experimental phenomena. These two models are used to calculate a molecule's CARS spectrum.

2.1. Harmonic Oscillator

To model the vibrational motion of a diatomic molecule, the molecule can be treated as two masses, m_1 and m_2 , separated by a spring with a force constant k . Each mass can be treated separately with their own equations of motion, however, by using the reduced mass of the molecule μ , we can treat the two-body problem

as a one-body problem with an equation of motion in one dimension of the form

$$\mu \frac{d^2x}{dt^2} + kx = 0. \quad (1)$$

The potential energy of this molecule is then

$$V(x) = \frac{1}{2}kx^2 \quad (2)$$

and by solving the Schrödinger equation in one-dimension with this potential

$$\frac{d^2\psi(x)}{dx^2} = \frac{2\mu \left(\frac{1}{2}kx^2 - E \right)}{\hbar^2} \psi(x), \quad (3)$$

we get well-behaved, finite solutions only when the energy is restricted to the form

$$E_v = \hbar \left(\frac{k}{\mu} \right)^{1/2} \left(v + \frac{1}{2} \right) \quad v = 0, 1, 2, \dots \quad (4)$$

where \hbar is the reduced Planck's constant and v is the vibrational quantum number. The vibrational energy is quantized as determined by v . A diatomic molecule can transition from one energy level, v , to another by absorbing or emitting radiation whose frequency satisfies the Bohr frequency condition, $\Delta E = h\nu_{\text{obs}}$, where Eq. (5) is the observed frequency that determines the spacing of energy levels.

$$\nu_{\text{obs}} = \frac{1}{2\pi} \left(\frac{k}{\mu} \right)^{1/2} \quad (5)$$

2.2. Rigid Rotator

A simple model for a rotating molecule, known as the rigid-rotator, is where two masses, m_1 and m_2 , are separated by a fixed distance r_1 and r_2 from its center of

mass. This is a good approximation even when considering vibrating diatomic molecules because the amplitude of vibrations is small compared to its bond length. The kinetic energy of the rotator rotating at a frequency of ν_{rot} cycles per second is then

$$K = \frac{1}{2}(m_1 r_1^2 + m_2 r_2^2)\omega^2 \quad (6)$$

where ω is the angular speed defined as $2\pi\nu_{\text{rot}}$. Like in the harmonic oscillator, the molecule can be treated as a one-body problem by using the reduced mass, μ , and the distance between the masses, $\vec{r} = \vec{r}_2 - \vec{r}_1$. By making these substitutions, Eq. (6) can be rewritten in terms of the molecule's moment of inertia, $I = \mu r^2$, and angular momentum, $L = I\omega$, as

$$K = \frac{L^2}{2I}. \quad (7)$$

In this case, the Hamiltonian operator equals the kinetic energy operator because the molecule's energy does not depend on its orientation due to a lack of external forces. The kinetic energy operator for the rigid-rotator is then

$$\hat{K} = \hat{H} = -\frac{\hbar^2}{2\mu}\nabla^2. \quad (8)$$

To solve the Schrödinger equation for the rigid rotator, it is useful to use the Laplacian operator in spherical coordinates. In the special case where the radius, r , is constant as in the rigid rotator approximation, we get the expanded form of Eq. (8) to be

$$\hat{H} = -\frac{\hbar^2}{2I} \left[\frac{1}{\sin \theta} \frac{\partial}{\partial \theta} \left(\sin \theta \frac{\partial}{\partial \theta} \right) + \frac{1}{\sin^2 \theta} \left(\frac{\partial^2}{\partial \phi^2} \right) \right] \quad (9)$$

and therefore the Schrödinger equation is

$$-\frac{\hbar^2}{2I} \left[\frac{1}{\sin \theta} \frac{\partial}{\partial \theta} \left(\sin \theta \frac{\partial}{\partial \theta} \right) + \frac{1}{\sin^2 \theta} \left(\frac{\partial^2}{\partial \phi^2} \right) \right] Y(\theta, \phi) = EY(\theta, \phi) \quad (10)$$

Multiplying Eq. (10) by $\sin^2 \theta$ and letting

$$\beta = \frac{2IE}{\hbar^2} \quad (11)$$

we get

$$\sin \theta \frac{\partial}{\partial \theta} \left(\sin \theta \frac{\partial Y}{\partial \theta} \right) + \frac{\partial^2 Y}{\partial \phi^2} + (\beta \sin^2 \theta) Y = 0 \quad (12)$$

The solutions to Eq. (12) are closely related to the orbitals of a hydrogen atom [5] and tell us that β must obey the following condition

$$\beta = J(J+1) \quad J = 0, 1, 2, \dots \quad (13)$$

From Eq. (11) and Eq. (13) we obtain an equation for discrete rotational energy levels

$$E_J = \frac{\hbar^2}{2I} J(J+1) \quad J = 0, 1, 2, \dots \quad (14)$$

2.3. Corrections to the Model

Disagreements exist between the theoretical spectra calculated with the above two models and the experimental data. Mainly, pure rotational spectral lines are not equally spaced as predicted due to the effects of vibrations on the rotational energies. Centrifugal distortions are also not considered in the rigid rotator model. This section introduces corrections to account for the rotational-vibrational interaction and centrifugal distortions.

The total rotational energy of a diatomic molecule with corrections for the rotational-vibrational interaction and centrifugal distortions is shown in Eq. (15).

$$F(J) = \tilde{B}_\nu J(J+1) - \tilde{D}_\nu J^2(J+1)^2 \quad (15)$$

The tildes on \tilde{B}_ν and \tilde{D}_ν signal that these coefficients, and therefore the total energy, are in units of cm^{-1} which are known as wavenumbers. Both coefficients in Eq. (15) are vibrational energy level-dependent as denoted by the ν subscripts. From Eq. (11) we see that B depends on the molecule's bond length from the dependence on the moment of inertia, I . In the first-order approximation, we took the bond length to be constant, however, as the vibrational amplitude increases, one can easily be convinced that the bond length should also slightly increase. With this increased bond length, B decreases. In Eq. (15), \tilde{D}_ν is known as the centrifugal distortion coefficient and its purpose is to account for the fact that a molecule's bond can stretch as it rotates. This causes the molecule to lose energy and is a more prominent effect at higher energy rotational states.

3. The Molecular Response Function

The molecular response function [4], Eq. (16), describes how each allowed transition contributes to the CARS signal. The following section contains a brief overview of this function and its components.

$$R_{\text{CARS}}(t) = \sum_\nu \sum_J I_{\nu,J;\nu,J+2} \times \exp \left[\frac{t}{\hbar} \left(i\Delta E_{\nu,J;\nu,J+2} - \frac{1}{2} \Gamma_{\nu,J;\nu,J+2}^S \right) \right] \quad (16)$$

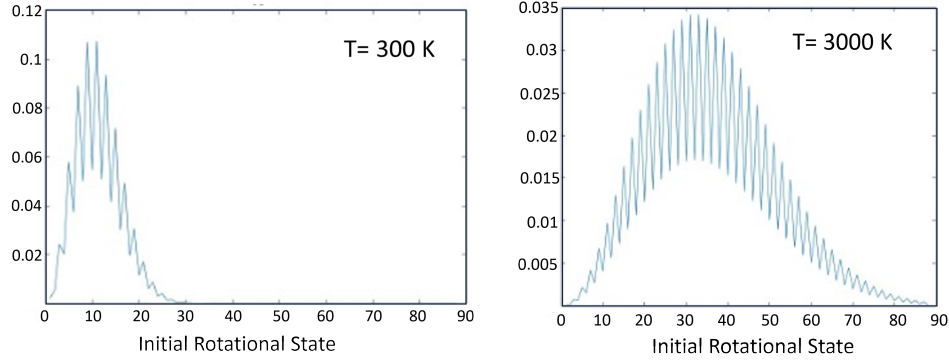


Fig. 1. The Boltzmann population distribution of rotational states initially populated at 300K and 3000K. At higher temperatures, more rotational states are populated due to the increased energy in the system.

3.1. Boltzmann-weighted transition strengths

The initial rotational state of all molecules in the sample is governed by the Boltzmann population distribution, which is heavily dependent on the temperature of the sample. The higher the temperature of a sample, the more rotational levels will be present, which can be seen in Fig. (1). This distribution is used to calculate the likelihood that a transition from one rotational state to the next will occur. The vibrational state of the molecules is assumed to be constant and uniform because only rotational energy levels are simulated for rotational CARS. In a later section, it will be shown that the user can set which vibrational state they would like to generate data for.

The Boltzmann-weighted transition strengths are proportional to the three terms in Eq. (17) below.

$$I_{v,J;v,J+2} \propto b_{J,J+2} \times F_{\text{rot}(J)} \times \Delta\rho_{v,J;v,J+2} \quad (17)$$

A transition from an initial rotational state J to an elevated rotational state,

$J+2$, is proportional to the difference in the Boltzmann population of rotational states J and $J+2$. This population difference is the $\Delta\rho_{v,J;v,J+2}$ term in Eq. (17). The $F_{\text{rot}(J)}$ are the Herman-Wallis factors for rotational state J and $b_{j,J+2}$ are the Placzek-Teller coefficients.

3.2. Additional Terms

Equation (18) is the difference in energy of an allowed transition from J to $J + 2$, where $F(J)$ is defined by Eq. 15.

$$\Delta E_{v,J;v,J+2} = F(J + 2) - F(J) \quad (18)$$

Equation (19) models the dephasing induced by the molecules colliding in the sample. It is computationally implemented based on the Modified Exponential Gap model for line mixing [6].

$$\Gamma_{v,J;v,J+2}^S \quad (19)$$

4. Results

The existing spectral library generation code was made up of many iterations. Each of these iterations were written for a different molecular species and had its functionality spread amongst multiple files. This required researchers to find the correct files for their specific experiments. Many experimental parameters that are commonly adjusted, such as temperature and concentration, were located in different files. This made adjusting these parameters tedious and not intuitive. It also proved to be difficult to share the correct code with colleagues and collaborators who requested certain versions for their experiments.

Additionally, researchers using the code for the first time would struggle to use it correctly. Overall, the organization and usability of the code needed to be improved. To remedy this, we consolidated all the existing code into a single, user-friendly Matlab App with a GUI. This organized the code base and now only one program can be universally shared to collaborators. The GUI solves the usability issues because users can now easily adjust all experimental parameters from one interface. Aside from creating a user-friendly experience, the program was also designed to be robust which assured that the program is accessible to users without the need for lengthy documentation or tutorials. The upcoming sections present pictures of the GUI and discuss the robust and flexible design of the program.

4.1. Robust Design

In the early stages of development, the program would crash if certain inputs were not given according to MATLAB's syntax rules. For example, the temperature and pressure ranges prompt the user for an initial, final, and step value and would crash if the final value was less than the initial value. Now if the user only inputs an initial and final value, the program will set those two values as the range, allowing the final value to be less than the initial value as well. Users also have the option to input a single value in the range field or select an option to input discrete values for these ranges. Many input formats are accommodated, and in certain cases where the program would still normally crash, a warning label is shown to the user within the interface.

Default values for all parameters are initially set to allow the program to run immediately after startup. Instead of leaving all values empty upon startup, for the sake of robustness, the program can be run without input from the user. One

downside to this is that the program will produce a CARS spectrum, even if a user forgets to change a certain parameter, which could produce misleading results. However, these default values can be easily changed from the program's code file by users. Other features that make the code robust include warning users if the concentrations of O₂ and N₂ in air don't add to 100% and if users enter a temperature or pressure range that doesn't include the value they specified as the upper limit due to the step size they inputted.

4.2. Flexibility

The number of available parameters to be set for each instance of library generation was vast. A table of parameters was created, Fig. (2), which enables the user

Parameters		
	Value	Units
Pump Delay	0	s
Probe Delay	6.5000e-10	s
Pump Freq	3.7474e+14	s-1
chirp_pump	0	s-2
chirp Stokes	0	s-2
chirp Probe	0	s-2
INR	1	unit
GammaINR	100	unit
Guass Param	1	unit
Slit Function Width	1	cm-1
Wave Number Max	250	cm-1
Wave Number Min	0	cm-1

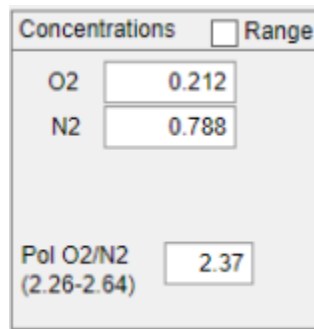
Fig. 2. A table of parameters was created to allow quick adjustments to common parameters. The table is loaded initially with default values but users can change any value they need to. This is a compact way to visualize what the parameters are set to and give users the option to adjust them.

to adjust parameters when needed. With this table, the user's flexibility was

increased, and prompting the user to specify each parameter was avoided if a default value was sufficient. One example of a parameter that can be adjusted in the table is the generated plots' minimum and maximum wave numbers. As temperatures increase, the Raman shifts grow larger and the wavenumber axis on the final plots needs to be adjusted to show the whole spectrum. In many low-temperature cases, the default values of 0 to 200 wavenumbers are sufficient, and prompting the user for these values every run would be unnecessary. Previously a user would have to sift through many files and lines of code to change these values.

Another feature that was implemented was different options according to the species selected. Species-specific parameters were implemented into the GUI, so depending on what species is selected, the user will be prompted to change the appropriate parameters. For example, when air is selected as the species, the option to input a range of O₂ concentrations is presented, Fig. (3), because in some experiments, the concentrations of O₂ in an air sample are unknown. Allowing users to sweep ranges of O₂ concentrations generates libraries of data that can then be fit to experimental data to determine the concentration in their sample. If a user decides to change their mind and select a different species after previously inputting parameters for the old species, those inputs will be remembered but not used. This allows the user to input all species-specific parameters before any code execution and then cycle through molecules after each execution without any additional inputs.

Other flexibility features were also implemented, such as allowing the user to change the output file path where the library data will be saved with a browse button or directly typing the path. Also, a reset button restarts the program with



Concentrations		<input type="checkbox"/> Range
O2	0.212	
N2	0.788	
Pol O2/N2 (2.26-2.64)	2.37	

Fig. 3. An option to include concentrations is presented when producing spectra for air. A warning pops up when the concentrations entered don't add to 100%. There is also support for a range of concentrations when the user would like each spectrum to have a different concentration.

the click of a button in cases where the user would like to reset all values to defaults. Another button allows users to clear all open plots, while, another button lets users disable plots from appearing at all. Advanced users can change the default values because they are assigned at the top of the program's code, allowing them to easily find where to change these values.

5. Discussion

Making the CARS modeling code user-friendly by creating a GUI increases the usability of the code and makes it easier for new researchers to generate the spectral libraries they need without a large learning curve. Having interns, post-docs, and new members be able to generate libraries on day one makes conducting experiments and analysis more efficient because they won't have to learn their way around the code. The GUI is designed to be robust such that new users aren't met with a program that crashes often and instead warns users of potential problems.

Our other task, aside from building a GUI, was to consolidate and adapt the code into a single program. This makes the distribution of the modeling code

easier because one program can be universally sent to collaborators and other researchers. Previously, only specific code files were sent for a researcher's experiments which means someone would have to determine the correct files to send. Since the code was adapted into a single program, it can now be sent to all researchers.

The increased usability and ease of distribution will make this new program highly sought-after and will prove to be a great tool for researchers in this field. However, more work can be done to improve the program, such as adding support for more molecular species, adding quality of life (QOL) features, and testing to ensure accuracy. Including support for additional molecular species will expand the number of researchers who could use the program. Since the program currently allows for the mixing of certain species, such as O₂ and N₂ for an air mixture, support for more molecular mixtures could be added. A main QOL feature that could be added to the GUI is allowing the name of the output file for each spectrum to be changed. Currently, the file is named using an automatic system that includes the molecule, temperature, pressure, vibrational state, and more. However, researchers would find it useful if they could change which parameters show up in the file name from the GUI instead of having to sift through the lines of code. Finally, additional testing is needed to ensure the accuracy of the spectra generated from the program. Spectra generated with high pressure tend to be inaccurate and additional testing is required to determine if this is due to the model or if it occurred by adapting the code into a single program. [7]

References

1. A. Bohlin, C. Jainski, B. D. Patterson, *et al.*, “Multiparameter spatio-thermochemical probing of flame–wall interactions advanced with coherent raman imaging,” *Proc. Combust. Inst.* **36**, 4557–4564 (2017).
2. H. U. Stauffer, J. D. Miller, M. N. Slipchenko, *et al.*, “Time- and frequency-dependent model of time-resolved coherent anti-Stokes Raman scattering (CARS) with a picosecond-duration probe pulse,” *The J. Chem. Phys.* **140**, 024316 (2014).
3. T. Y. Chen, S. A. Steinmetz, B. D. Patterson, *et al.*, “Direct observation of coherence transfer and rotational-to-vibrational energy exchange in optically centrifuged co₂ super-rotors,” *Nat. Commun.* **14** (2023).
4. T. Y. Chen and C. J. Kliewer, “Numerical study of pure rotational fs/ps cars coherence beating at high pressure and for multi-species rotation-vibration non-equilibrium thermometry,” *The J. Chem. Phys.* **157**, 164201 (2022).
5. D. A. McQuarrie and J. D. Simon, *Physical Chemistry: A Molecular Approach* (University Science Books, Sausalito, CA, 1997).
6. C. J. Kliewer, A. Bohlin, E. Nordström, *et al.*, “Time-domain measurements of s-branch N₂–N₂ raman linewidths using picosecond pure rotational coherent anti-stokes raman spectroscopy,” *Appl. Phys. B* **108** (2012).
7. T. Y. Chen, C. J. Kliewer, B. M. Goldberg, *et al.*, “Time-domain modelling and thermometry of the ch₄ 1 q-branch using hybrid femtosecond/picosecond coherent anti-stokes raman scattering,” *Combust. Flame* **224**, 183–195 (2021). A dedication to Professor Ronald K. Hanson.